Proceedings of *RAGtime 23–25*
Z. Stuchlík, G. Török, V. Karas and D. Lančová, editors, Silesian University in Opava, 2023, pp. 93–107

Non-conducting tori around black hole immersed in parabolic magnetic field

Martin Blaschke[1,a] Zdeněk Stuchlík[1] Jiří Kovář[1] and Petr Slaný[1]

[1]Research Centre for Theoretical Physics and Astrophysics,
Institute of Physics, Silesian University in Opava.
Bezručovo náměstí 13, CZ-746 01 Opava, Czech Republic
[a]martin.blaschke@physics.slu.cz

ABSTRACT
We study charged fluid tori with vanishing conduction current orbiting in the background given by a Schwarzschild black hole immersed in a parabolic magnetic field introduced in the context of the Blandford-Znajek process. In our study, we focus on the off-equatorial charged tori that could be related to the creation of jets due to the Blandford-Znajek process.

Keywords: Black holes – parabolic magnetic field – general relativity

1 INTRODUCTION

Accretion disks orbiting a central black hole are assumed as engines of active galactic nuclei with central supermassive black holes, or microquasars in binary systems containing a stellar-mass black hole (Abramowicz and Fragile, 2013a). The extraordinary energy outputs observed in such objects are related to the radiation of the disks and the related jets. Basically, accretion disks are modeled as geometrically thin Keplerian accretion disks governed mainly by the spacetime circular geodesics (Novikov and Thorne, 1973), or as geometrically thick accretion disks governed by the Euler equation and the related effective potential reflecting the interplay of the gravitational and inertial forces with the pressure gradients (Kozlowski et al., 1978; Stuchlík et al., 2000). Closed equipotential surfaces of the effective potential govern equilibrium tori, accretion (excretion) tori are governed by self-crossing equipotential surfaces; open equipotential surfaces govern jets. Complex equatorial toroidal structures, named ringed accretion disks, orbiting Kerr black holes and describing simultaneously relatively counter-rotating tori were introduced in Pugliese and Stuchlík (2015, 2016, 2017, 2018); Pugliese and Stuchlik (2019). The jets are usually modeled in the framework of the Blanford-Znajek process that involves electromagnetic fields external to the black hole and generated by electric currents in the accretion disks (Blandford and Znajek, 1977).

978-80-7510-577-6

The electromagnetic fields external to the central black hole are generally very important both for the behavior of the accretion disks and the creation of related jets. Recently, it has been demonstrated that the external magnetic field strongly influences ionized Keplerian disks, causing their transformation to thick disks or leading, in extreme cases, to their destruction Kološ et al. (2015); Stuchlík and Kološ (2016); Tursunov et al. (2016); Pánis et al. (2019); Stuchlík et al. (2019). In complex general-relativistic magneto-hydrodynamic approach Gammie et al. (2003); Komissarov (2004); Tchekhovskoy et al. (2008) describing simultaneously the disks and the jets, fluid plasma structures are usually studied in the force-free approximation corresponding to infinite conductivity – for recent comments on the relation of the Blandford–Znajek process and the magnetic Penrose process (see Dadhich et al. (2018); Stuchlík et al. (2020)).

Existence of non-equatorial charged-particle circular orbits in the external magnetic fields around black holes (Kovář et al., 2008; Kovář et al., 2010; Kopáček et al., 2010) inspired idea of charged "non-conducting (more precisely: with vanishing conduction current)" fluid structures treated in an approximation of zero conductivity, representing a direct of usually used approximation of infinite conductivity. The model of charged non-conducting tori was introduced in Kovář et al. (2011) and further developed in Slaný et al. (2013); Cremaschini et al. (2013); Kovář et al. (2014); Kovář et al. (2016); Trova et al. (2018); Schroven et al. (2018). Such tori can be equatorial, but also can be off-equatorial, levitating outside the equatorial plane due to the electromagnetic interaction of the fluid charge with the magnetic field.

The magnetic field external to the black hole can be an external galactic magnetic fields amplified in the black hole's strong gravity, or a black hole can be immersed in the extremely strong magnetic field of a magnetar (Kovář et al., 2014). Of course, the accretion disk itself is constituted of conducting plasma that can create electric flows that can generate a magnetic field external to the black hole, as assumed in the Blandford-Znajek process.

The basic and simplest approximation of the magnetic fields is the uniform magnetic field introduced by Wald (Wald, 1974). The charged non-conducting tori were studied in the Kerr (Schwarzschild) black hole spacetimes and the uniform or dipole external magnetic fields (Slaný et al., 2013; Kovář et al., 2014), moreover, the off-equatorial tori having sufficiently low density can be considered as collision-less plasma (Cremaschini et al., 2013).

However, of special interest is the possibility of the existence of the off-equatorial non-conducting charged tori in the magnetic fields generated in the accretion disks, creating jets due to the Blandford-Znajek process that are thus also of direct astrophysical relevance. The split-monopole magnetic field generated by currents in thin accretion disks introduced in the first treatment of the Blandford-Znajek process (Blandford and Znajek, 1977), and confirmed as physically relevant by magneto-hydro-dynamic models (Komissarov, 2004), has been studied for the off-equatorial charged tori in Stuchlík et al. (2022).

Here, we focus attention on the possible existence of the off-equatorial charged tori in the parabolic magnetic field treated as a second possibility for the generation of jets in Blandford and Znajek (1977). The relevance of the parabolic field in the vicinity of the black holes is supported by recent numerical general relativistic magneto-hydrodynamic models of thick accretion disks, indicating that the evolution of the tori immersed initially

in any magnetic field results in a final state with a parabolic field located outside the torus near the rotation axis of the system (Tchekhovskoy et al., 2008).

We first present basic ideas of the model of the charged non-conducting fluid structures and then investigate the existence and properties of the charged tori around Schwarzschild black holes surrounded by the parabolic magnetic field that can be considered as a simple but realistic approximation of the electromagnetic fields. We use the geometric unit with $c = G = 1$.

2 MODEL OF CHARGED FLUID TORI

We assume a stationary and axisymmetric background field composed of gravitational, $g_{\alpha\beta}$, and electromagnetic, $F_{\alpha\beta} = \nabla_\alpha A_\beta - \nabla_\beta A_\alpha$, parts. Test configurations of a perfect fluid with charge density q_ρ, energy density ϵ and pressure p allowing their orbiting in the fixed background. The considered background fields and the charged configurations have a common axis. Under the presented assumptions, the equilibrium charged fluid configurations are determined by the general energy-momentum conservation law

$$\nabla_\beta \mathcal{T}^{\alpha\beta} = 0, \tag{1}$$

where the energy-momentum tensor $\mathcal{T}^{\alpha\beta} = T^{\alpha\beta} + T^{\alpha\beta}_{\rm em}$ with its parts

$$T^{\alpha\beta} = (\epsilon + p)U^\alpha U^\beta + p g^{\alpha\beta}, \tag{2}$$

$$T^{\alpha\beta}_{\rm em} = \frac{1}{4\pi}\left(\mathcal{F}^\alpha{}_\gamma \mathcal{F}^{\beta\gamma} - \frac{1}{4}\mathcal{F}_{\gamma\delta}\mathcal{F}^{\gamma\delta} g^{\alpha\beta}\right), \tag{3}$$

describes charged fluid with negligible viscosity and heat conduction. The general electromagnetic part of this tensor is related to the Faraday tensor having two parts, $\mathcal{F}^{\alpha\beta} = F^{\alpha\beta} + F^{\alpha\beta}_{\rm self}$, where the background and the self electromagnetic components satisfy the Maxwell equations

$$\nabla_\beta F^{\alpha\beta} = 0, \quad \nabla_\beta F^{\alpha\beta}_{\rm self} = 4\pi J^\alpha, \tag{4}$$

with the four-current density field of the charged fluid J^α satisfying the general Ohm law

$$J^\alpha = q_\rho U^\alpha + \sigma F^{\alpha\beta} U_\beta. \tag{5}$$

Usually, the so-called force-free model assumes that the conductivity $\sigma \to \infty$ is applied for the description of the phenomena around the black holes (see, e.g., Blandford and Znajek, 1977). The dynamics of the charged matter is then governed by the force-free relation $F^{\alpha\beta}U_\beta = 0$, and the inertia of the matter is fully abandoned. Then, the first term of the right-hand side of the Ohm law is not considered. In the model of non-conducting charged fluids, assuming $\sigma \to 0$, the situation is inverse, and the second term in the Ohm law is abandoned – in this approach, it is thus supposed that the electric charges are fixed to the rotating matter. The assumption of vanishing conductivity is necessary for the self-consistency of the axial symmetry of the model of charged fluid tori, as a non-zero conductivity implies

due to the Ohm law existence of radial electric flows – for details see Kovář et al. (2016) (of course, the inclusion of both the terms in the right-hand side of the Ohm law implies complex configurations including the conducting electric flows and possible strong self-electromagnetic fields). The charged non-conducting fluid tori are then governed by the so-called "master equation" (Kovář et al., 2011)

$$\nabla_\beta T^{\alpha\beta}_{\text{fluid}} = F^{\alpha\beta}_{\text{ext}} J_\beta, \tag{6}$$

where $F^{\alpha\beta}_{\text{ext}}$ denotes the background electromagnetic field that can be of internal origin being related directly to the black hole as in the case of the Kerr-Newman (Reissner–Nordström) backgrounds, or can be of external origin being related to the Kerr (Schwarzschild) gravitational backgrounds as is the case of our study; the basic differences between the internal and external fields are discussed in Stuchlík et al. (2019). The master equation determines the balance equations of the orbiting charged non-conducting fluid. In the following we simplify notation to $F^{\alpha\beta}_{\text{ext}} = F^{\alpha\beta}$.

2.1 Balance equations of the equilibrium fluid configurations

The basic features of the charged fluid model can be summarized as follows. The elementary charges in the fluid are adherent to the fluid elements, i.e. we assume $\sigma = 0$; the charged elements are uniformly rotating in the azimuthal direction with the four-velocity field $U^\alpha = (U^t, 0, 0, U^\phi)$ and $U^\alpha \neq U^\alpha(t, \phi)$. Moreover, presuming the electromagnetically test fluid, $F^{\alpha\beta}_{\text{self}} \ll F^{\alpha\beta}$, the general energy-momentum conservation law (1) reduces to the final form (Kovář et al., 2011)

$$\nabla_\beta T^{\alpha\beta} = F^{\alpha\beta} J_\beta, \tag{7}$$

governing the orbiting charged non-conducting fluid. The related fluid-flow pressure balance equations take the form

$$\begin{aligned} \partial_r p &= -(p+\epsilon)\mathbb{R}^\circ + q_\rho \mathbb{R}^* \equiv \mathbb{R}, \\ \partial_\theta p &= -(p+\epsilon)\mathbb{T}^\circ + q_\rho \mathbb{T}^* \equiv \mathbb{T}. \end{aligned} \tag{8}$$

The right-hand sides of the equations governing the pressure gradients guaranteeing the fluid balance are denoted as $\mathbb{R} = \mathbb{R}(r, \theta)$ and $\mathbb{T} = \mathbb{T}(r, \theta)$, and are separated them into two parts – the hydrodynamical, and the additional electro-magneto-hydrodynamical that are given by the relations

$$\begin{aligned} \mathbb{R}^\circ &= \partial_r \ln|U_t| - \frac{\Omega \partial_r \ell}{1-\Omega\ell}, \quad \mathbb{R}^* = U^t \partial_r A_t + U^\phi \partial_r A_\phi, \\ \mathbb{T}^\circ &= \partial_\theta \ln|U_t| - \frac{\Omega \partial_\theta \ell}{1-\Omega\ell}, \quad \mathbb{T}^* = U^t \partial_\theta A_t + U^\phi \partial_\theta A_\phi. \end{aligned}$$

The standard fluid models of toroidal configurations (Kozlowski et al., 1978; Stuchlík et al., 2000) are governed by the pure hydrodynamical parts $\mathbb{R}^\circ$ and $\mathbb{T}^\circ$.

The specific angular momentum profile of the rotating fluid, $\ell = -U_\phi/U_t$, and the angular velocity related to the static distant observers, $\Omega = U^\phi/U^t$, are related by the formula

$$\Omega = -\frac{\ell g_{tt} + g_{t\phi}}{\ell g_{t\phi} + g_{\phi\phi}}. \tag{9}$$

The profile of the time component of the four-velocity U_t can be expressed as

$$(U_t)^2 = \frac{g_{t\phi}^2 - g_{tt}g_{\phi\phi}}{\ell^2 g_{tt} + 2\ell g_{t\phi} + g_{\phi\phi}} = \frac{g_{t\phi}^2 - g_{tt}g_{\phi\phi}}{g_{tt} + 2\Omega g_{t\phi} + \Omega^2 g_{\phi\phi}}\,. \tag{10}$$

The axial component of the four-velocity field is then given by the relation $U_\phi = -\ell U_t$. Derivation of the pressure equations (8) can be found in Kovář et al. (2011); Kovář et al. (2014); Kovář et al. (2016); their uncharged limit $q_\rho = 0$ corresponds to the Euler equation describing a rotating electrically neutral perfect fluid (Kozlowski et al., 1978; Abramowicz et al., 1978a; Stuchlík, 2005; Stuchlík et al., 2009).

The specific angular momentum ℓ profile, the angular velocity Ω profile, and the charge density profile are linked due to the relation

$$\partial_\theta \mathbb{R} + \mathbb{T}\partial_p \mathbb{R} = \partial_r \mathbb{T} + \mathbb{R}\partial_p \mathbb{T}, \tag{11}$$

i.e., the integrability condition of the pressure balance equations (8); the profiles $q_\rho = q_\rho(r,\theta)$ and $\ell = \ell(r,\theta)$ ($\Omega = \Omega(r,\theta)$) have to be adjusted to each other in accord with this condition. To close the system of equations, we assume perfect fluid governed by the polytropic equation of state, with the polytropic energy density, rest energy density and pressure related by equations

$$p = \kappa\rho^\Gamma, \quad \epsilon = \rho + \frac{1}{\Gamma - 1}p, \tag{12}$$

where κ and Γ denote the polytropic coefficient and exponent.

2.1.1 Intergal analytical solution of the pressure balance equations

For the charged non-conducting fluids, we can make a significant simplification, enabling even analytic integration of the balance pressure equations. By introducing the charge density transformation

$$\mathcal{K} = \frac{q_\rho}{\epsilon + p}U^\phi, \tag{13}$$

and the pressure transformations

$$\partial_r w = \frac{\partial_r p}{(p+\epsilon)}, \quad \partial_\theta w = \frac{\partial_\theta p}{(p+\epsilon)}, \tag{14}$$

and the electromagnetic vector time component transformation relations

$$\partial_r a_t = \Omega^{-1}\partial_r A_t, \quad \partial_\theta a_t = \Omega^{-1}\partial_\theta A_t\,, \tag{15}$$

we arrive to the transformed pressure balance equations

$$\partial_r w = -\partial_r \ln|U_t| + \frac{\Omega\partial_r\ell}{1-\Omega\ell} + \mathcal{K}\partial_r A,$$
$$\partial_\theta w = -\partial_\theta \ln|U_t| + \frac{\Omega\partial_\theta\ell}{1-\Omega\ell} + \mathcal{K}\partial_\theta A, \tag{16}$$

where $\partial_r A = \partial_r a_t + \partial_r A_\phi$ and $\partial_\theta A = \partial_\theta a_t + \partial_\theta A_\phi$, enabling a unification. That is, if the barotropic fluid is considered, having $\epsilon = \epsilon(p)$ guaranteed by the chosen polytropic equation of state (12), the fluid rotation regime and charged density chosen so that $\Omega = \Omega_1(\ell)$, $\Omega = \Omega_2(A_t)$ and $\mathcal{K} = \mathcal{K}(A)$, we can join the system of equations (16) into the unified integral form

$$\int_0^w \mathrm{d}w = -\ln\left|\frac{U_t}{U_{t_{\rm in}}}\right| + \int_{\ell_{\rm in}}^{\ell}\frac{\Omega\mathrm{d}\ell}{1-\Omega\ell} + \int_{A_{\rm in}}^{A}\mathcal{K}\mathrm{d}A\,, \tag{17}$$

with the solution written in the form

$$w = \int_0^w \mathrm{d}w = -W + W_{\rm in}\,. \tag{18}$$

The function $W(r,\theta)$ is the effective potential (variable part of the right-hand side of equation (17)), and the subscript 'in' represents the inner edge of the orbiting fluid structure at $r = r_{\rm in}$ for $\theta = \theta_{\rm in}$, whereas for a function $X = X(r,\theta)$, we denote $X_{\rm in} = X(r_{\rm in},\theta_{\rm in})$ governing the constant of integration $W_{\rm in}$.

Due to pressure transformation relations (14) integrated to give

$$\int_0^w \mathrm{d}w = \int_0^p \frac{\mathrm{d}p}{p+\epsilon}, \tag{19}$$

the equipressure surfaces, $p = \text{const}$, determining the topology of the orbiting fluid structure coincide with the equipotential surfaces, $W = \text{const}$. It is well known that the effective potential governs all relevant aspects of the behavior of the stationary and axisymmetric fluid configurations both for uncharged fluids (Abramowicz et al., 1978b; Stuchlík et al., 2009) and for charged non-conducting fluids (Kovář et al., 2014; Kovář et al., 2016).

3 BLACK HOLES SURROUNDED BY PARABOLIC MAGNETIC FIELD

We focus here on the charged, non-conducting fluid circling in the background given by the static Schwarzschild black hole immersed in the parabolic magnetic field considered as a test field that is not influencing the spacetime. The Schwarzschild black holes are represented by the vacuum geometry with the line element taking the form (in the geometric units $c = G = 1$)

$$\mathrm{d}s^2 = g_{tt}\mathrm{d}t^2 + g_{rr}\mathrm{d}r^2 + g_{\theta\theta}\mathrm{d}\theta^2 + g_{\phi\phi}\mathrm{d}\phi^2, \tag{20}$$

where

$$g_{\theta\theta} = r^2\,, \quad g_{\phi\phi} = r^2\sin^2\theta\,, \quad g_{tt} = -f(r)\,, \quad g_{rr} = \frac{1}{f(r)}\,, \tag{21}$$

and the lapse function

$$f(r) = 1 - \frac{2M}{r}\,. \tag{22}$$

M denotes the black hole mass. For simplicity, we will use, in the following, the dimensionless coordinates ($r = r/M, t = t/M, s = s/M$) that are equivalent to using $M = 1$.

The parabolic magnetic field was introduced in Blandford and Znajek (1977) for modeling the creation of jets in the magnetosphere of the rotating black holes in the regions close to their horizon. The physical relevance of such a special kind of magnetic field was confirmed by numerical, fully general relativistic models of magneto-hydrodynamic processes around black holes, where it has been demonstrated that evolution of a thick accretion disk (toroid) under influence of various external magnetic fields (uniform, dipole, parabolic) always results in a final configuration having the magnetic field exterior to the toroidal configuration and close to the rotation axis of the black hole and torus system of the parabolic character (Tchekhovskoy et al., 2008).

For completeness, we also add the case of parabolic magnetic field as magneto-hydrodynamic fluid models of thick accretion disks orbiting a black hole demonstrate the final creation of a parabolic magnetic field near the rotation axis of the orbiting matter independently of the original configuration of the external magnetic field (Nakamura et al., 2018). The parabolic magnetic field predicted by some magnetohydrodynamic simulations is determined by the four-vector electromagnetic potential (Nakamura et al., 2018).

In the static Schwarzschild vacuum spacetimes, the parabolic magnetic field is static and axially symmetric, it thus has not the spherical symmetry of the Schwarzschild spacetime as is the case of the split monopole magnetic field; its $four-vector$ electromagnetic potential has thus the only non-zero component

$$A_\mu = (0, 0, 0, A_\phi), \tag{23}$$

and the axial component reads

$$A_\phi = \frac{g}{2} r\,(1 - \cos\theta) + 2M\,(1 + \cos\theta)\,[1 - \ln\,(1 + \cos\theta)]\,, \tag{24}$$

where the parameter g governs the intensity of the magnetic field and is directly related to the intensity of the electric current generating the magnetic field – for details as the asymptotic behaviour at the horizon and weak-field limit see Blandford and Znajek (1977).

Commonly used approximation to Eq. (24) is given by Crinquand et al. (2020); McKinney and Narayan (2007a,b)

$$A_\phi = \frac{g}{2} r^k\,(1 - |\cos\theta|)\,, \tag{25}$$

where $k \in [0; 1.25]$ is declination of magnetic field lines. The split monopole solution (Blandford and Znajek, 1977; Stuchlík et al., 2022) corresponds to $k = 0$ and Blandford-Znajeck paraboloidal model to $k = 1$. Mostly used value for the black hole magnetosphere in the jet funnel is $k = 3/4$ (Nakamura et al., 2018; Stuchlík et al., 2019).

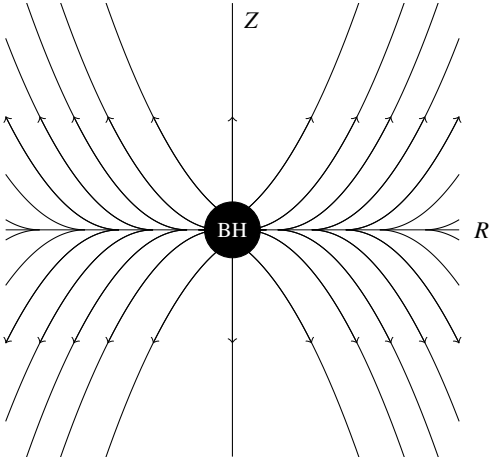

Figure 1. Scheme of a parabolic magnetic field in cylindrical coordinates given by Eq. (37).

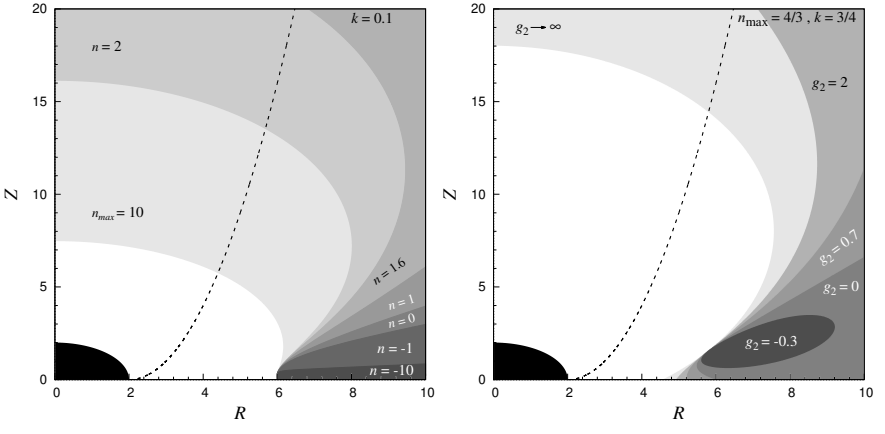

Figure 2. **Left:** Regions supporting minima of potential W under monomial ℓ =const. model. Parameter n spans from -10 to $n_{\max} \equiv 1/k$, i.e. the maximal value of this parameter consistent with physical potential ($\partial W/\partial r \to 0$ as $r \to \infty$). **Right:** Regions supporting minima of polynomial potential W under polynomial ℓ =const. model. In the figures, we have depicted the behaviour of parameter $n_{\max} \equiv 1/k$. We see that regions supporting the existence of minima are generally enlarged due to the non-zero g_2 constant. Also, that minima can now go under $R = 6$. We also see strange effects. For negative values of g_2, equatorial structures are suppressed. For thick discs, the model is relevant only above the dashed line, but for thin disks, it is relevant everywhere.

4 CHARGE TORI AROUND BLACK HOLES IN PARABOLIC MAGNETOSPHERE

In the Schwarzschild spacetimes, the four-velocity components satisfy the relations $U^t = g^{tt}U_t\,, U^\phi = g^{\phi\phi}U_\phi$ and the relation for the energy of the orbiting element simplifies to

$$(U_t)^2 = \frac{-g_{tt}g_{\phi\phi}}{\ell^2 g_{tt} + g_{\phi\phi}} = -\frac{f(r)r^2\sin^2\theta}{\ell^2 f(r) - r^2\sin^2\theta}. \tag{26}$$

The condition $(U_t)^2 > 0$ requires $\ell^2 g_{tt} + g_{\phi\phi} > 0$, implying the restriction on the acceptable values of the specific angular momentum in the form

$$\ell^2 < \frac{r^3\sin^2\theta}{r-2} \equiv l^2_{\rm ph}(r,\theta). \tag{27}$$

The function $l^2_{\rm ph}(r;\theta=\pi/2)$ governs the motion of photons in the equatorial plane, and for $l^2 = 27$ we obtain the circular photon orbit at $r = 3$ that represents the innermost limit on the position of circular geodesics.

Due to the simple form of the vector potential (23), the transformed pressure balance equations (16) reduce to the form

$$\begin{aligned}
\partial_r w &= -\,\partial_r \ln|U_t| + \frac{\Omega\partial_r\ell}{1-\Omega\ell} + \mathcal{K}\partial_r A_\phi,\\
\partial_\theta w &= -\,\partial_\theta \ln|U_t| + \frac{\Omega\partial_\theta\ell}{1-\Omega\ell} + \mathcal{K}\partial_\theta A_\phi,
\end{aligned} \tag{28}$$

whereas we require $\Omega = \Omega(\ell)$ and $\mathcal{K} = \mathcal{K}(A_\phi)$ for the integrability. Thus, the solution can be written in the form

$$w = -\ln\left|\frac{U_t}{U_{t_{\rm in}}}\right| + \int_{\ell_{\rm in}}^{\ell}\frac{\Omega{\rm d}\ell}{1-\Omega\ell} + g\int_{A_{\phi_{\rm in}}}^{A_\phi}\mathcal{K}\,{\rm d}A_\phi = -W + W_{\rm in}. \tag{29}$$

Below we demonstrate the existence of the off-equatorial tori, with their centers, possibly located at $(r_{\rm c},\theta_{\rm c})$, corresponding to local minima of the effective potential W (maxima of the pressure p). Thus, these locations must satisfy the necessary conditions

$$\partial_r W|_{\substack{r=r_{\rm c}\\ \theta=\theta_{\rm c}}} = 0, \quad \partial_\theta W|_{\substack{r=r_{\rm c}\\ \theta=\theta_{\rm c}}} = 0, \tag{30}$$

and, moreover, the sufficient conditions

$$\partial^2_{\theta\theta} W|_{\substack{r=r_{\rm c}\\ \theta=\theta_{\rm c}}} > 0, \quad \det\mathcal{H}|_{\substack{r=r_{\rm c}\\ \theta=\theta_{\rm c}}} > 0, \tag{31}$$

where

$$\mathcal{H} = \begin{pmatrix} \partial^2_{rr}W & \partial^2_{r\theta}W \\ \partial^2_{\theta r}W & \partial^2_{\theta\theta}W \end{pmatrix}, \tag{32}$$

[t]

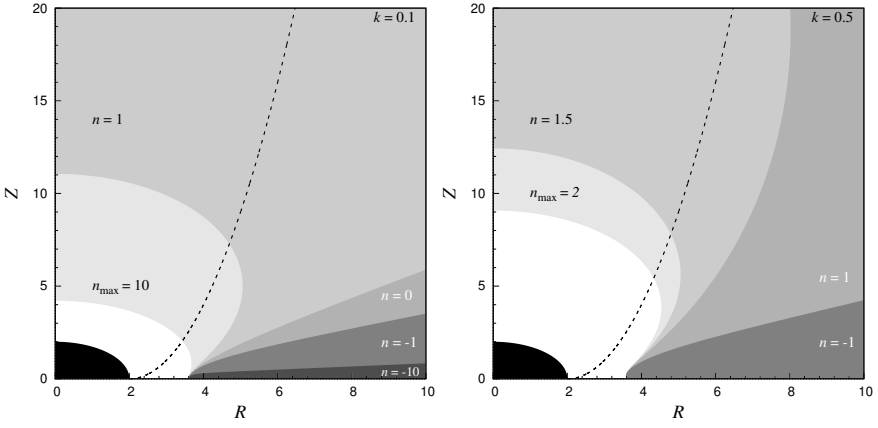

Figure 3. Regions supporting minima of potential W under monomial $\Omega = \ell^2/K$ model. Parameter n spans from -10 to $n_{\max} \equiv 1/k$, i.e. maximal value of this parameter consistent with physical potential ($\partial W/\partial r \to 0$ as $r \to \infty$). For thick discs, the model is relevant only above the dashed line, but for thin disks, it is relevant everywhere.

is the Hessian matrix. We survey a couple of rotation regimes of the fluid, particularly the case $\ell = \text{const.}$ and two cases $\ell \neq \text{const.}$ satisfying the condition $\Omega = \Omega(\ell)$, and the distribution of the charge density given by the monomial profile of the function $\mathcal{K} = \mathcal{K}(A_\phi)$, integrated as

$$\int \mathcal{K}\, \mathrm{d}A_\phi = g r^{kn} (1 - \cos\theta)^n \,, \tag{33}$$

for $n \neq 0$, relaxing the integration constants. For simplicity's sake, we consider cases $n = 0$ as a limiting case to avoid explicit logarithmic functions.

We also survey Polynomial regimes in the form

$$\int \mathcal{K}\, \mathrm{d}A_\phi = g r^{kn} (1 - \cos\theta)^n + g_2 r^{k(n-1)} (1 - \cos\theta)^{n-1} \,, \tag{34}$$

for $n \neq 0$ and $n \neq 1$ to again avoid explicit logarithmic functions.

4.1 Rotation regime $\ell = \text{const.}$

The rotation regime $\ell = \text{const}$ is a unique one, representing the marginally stable distribution of ℓ that is able to govern the basic properties of general acceptable equilibrium tori (Abramowicz and Fragile, 2013b). The potential given by Eg. (29), governing the toroidal configurations, takes under our assumptions form

$$W = \ln|U_t| - g r^{kn} (1 - \cos\theta)^n \,, \tag{35}$$

where we neglect the integration constant and consider the upper plane only, i.e. $\theta \in [0, \pi/2]$.
The necessary conditions (30) implying the set of equations (for any n)

$$g = \frac{\cos\theta_c \left(r_c^k \sin^2\frac{\theta_c}{2}\right)^{-n}}{3 - r_c + (3 - r_c + k(r_c - 2))\cos\theta_c},$$
$$\ell^2 = \frac{r_c^3 \sin^2\theta_c}{(r_c - 2)^2\left(1 - k\cot\theta_c \tan\frac{\theta_c}{2}\right)}. \tag{36}$$

These equations determine regions where a minimum of W exists. For picturing these regions and corresponding potentials W, it is more convenient to use cylindrical coordinates

$$R = r\sin\theta, \quad Z = r\cos\theta. \tag{37}$$

Regions are depicted in the left part of Fig. 2 where we have depicted the regions supporting minima of potential W under monomial ℓ =const. model. Here the parameter n spans from -10 to $n_{\max} \equiv 1/k$, i.e. the maximal value of this parameter consistent with physical potential ($\partial W/\partial r \to 0$ as $r \to \infty$). The model is only relevant for thick discs above the dashed line but for thin disks everywhere.

4.2 Polynomial potential

In the last section, we have seen that monomial potential might be too simple to support the effect on broad ranges of parameter k. Since we are interested in the minima of the potential W, let us introduce the polynomial character to it in the hope that a more complicated function would bring more minima points in the potential.

Therefore, let us explore the potential W in the polynomial form:

$$W = \ln|U_t| - g r^{kn}(1 - \cos\theta)^n - g_2 r^{k(n-1)}(1 - \cos\theta)^{(n-1)}, \tag{38}$$

where g_2 is another constant.

The example behaviour of this potential can be seen in the right part of Fig. (2). Here, we can see that the constant g_2 generally enlarges the areas where the potential W admit the existence of minima.

4.3 Rotation regime Ω = const.

Let us consider another very elemental regime with constant Ω. The potential is given by the relation

$$W = \ln|U_t| + \ln|1 - \Omega\ell| - g r^{kn}(1 - \cos\theta)^n. \tag{39}$$

Here ℓ is given by Eq. (10) and it is equal to

$$\ell = \Omega\frac{r^2\sin^2\theta}{f(r)}. \tag{40}$$

Due to the necessary conditions (30), in the centers of the toroidal structures, the constant Ω takes value

$$\Omega_{\rm c}^2 = \frac{1}{r_{\rm c}^3 \sin\theta_{\rm c}\left(\sin\theta - k\cos\theta\tan\frac{\theta}{2}\right)} \tag{41}$$

and the constant g takes the same form as was given in the previous case by Eq. (36).

However, putting all these conditions into effective potential, we can see that for any profile of the function $\mathcal{K}$, there are no possible centres of the toroidal structures. This result is consistent with findings in Stuchlík et al. (2022).

4.4 Rotation regime $\Omega \sim \ell^2$.

The integrability condition $\Omega(\ell)$ restricts possible choices of angular velocity. The choice

$$\Omega = \frac{\ell^2}{K}, \tag{42}$$

where K is an arbitrary non-zero constant, is equivalent via eq. (10) to

$$\ell = K\frac{f(r)}{r^2\sin^2\theta}, \tag{43}$$

usually supports the existence of an off-equatorial minimum in potential W. The potential is given by the relation

$$W = \ln|U_t| + \ln\left|1 - \frac{K^2 f^3(r)}{r^6\sin^6\theta}\right| - gr^{kn}(1-\cos\theta)^n\ . \tag{44}$$

The center is given by the same g as in eq. (36) and by

$$K = \frac{r_{\rm c}^{\frac{5}{2}}\sin^3\theta_{\rm c}}{f^2(r_{\rm c})\sqrt{1 - k\cot(\theta)\tan\left(\frac{\theta}{2}\right)}}\,. \tag{45}$$

The example behaviour of this potential can be seen in Fig. (3), where we have depicted the regions supporting minima of potential W under the monomial $\Omega = \ell^2/K$ model. Here, the parameter n spans from -10 to $n_{\rm max} \equiv 1/k$, i.e. the maximal value of this parameter consistent with physical potential ($\partial W/\partial r \to 0$ as $r \to \infty$). For thick discs, the model is relevant only above the dashed line, but for thin disks, it is relevant everywhere.

5 CONCLUSIONS

In modeling jets created by the Blandford-Znajek process, the one of assumed magnetic field has the character of the parabolic field.

We have demonstrated the existence of nonconducting charged tori located off the equatorial plane for properly chosen parameters governing their location and structure; namely, the distribution of the specific angular momentum, and the electric charge density.

We conclude that we were able to demonstrate clearly existence of nonconducting charged tori created by heavy particles located off the equatorial plane that could be, under the properly chosen condition on the charged matter, its distribution, and distribution of the specific angular momentum governing their equilibrium configurations, allowed to occur near the symmetry axis of the magnetized black hole. The charged tori is located near the symmetry axis could represent a possible obstacle for the matter of the jets that should probably interact with such configurations–the accelerated electrons should collide with heavy particles constituting the charged tori. Interactions of extremely accelerated electrons of the jet with the equilibrium tori created by heavy particles should lead to specific effects that could be observed and maybe to some modifications of the Blandford–Znajek process. Clearly, the phenomenon of charged nonconducting tori located near the symmetry axis would be a serious challenge for future research in the field of accretion disks and related jets.

ACKNOWLEDGEMENTS

The authors thanks the referee for careful reading of the original version of the manuscript. The work was supported by Institute of Physics in Opava. We also thank the internal grant of Silesian University, SGS/30/2023: Dynamics of structures in strong gravomagnetic fields of compact objects modeled in the framework of Einstein or alternative theories of gravity.

REFERENCES

Abramowicz, M., Jaroszynski, M. and Sikora, M. (1978a), Relativistic, accreting disks., *A&A*, **63**, pp. 221–224.

Abramowicz, M., Jaroszynski, M. and Sikora, M. (1978b), Relativistic, accreting disks, *A&A*, **63**, pp. 221–224.

Abramowicz, M. A. and Fragile, P. C. (2013a), Foundations of Black Hole Accretion Disk Theory, *Living Reviews in Relativity*, **16**(1), 1, arXiv: 1104.5499.

Abramowicz, M. A. and Fragile, P. C. (2013b), Foundations of Black Hole Accretion Disk Theory, *Living Reviews in Relativity*, **16**(1), 1, arXiv: 1104.5499.

Blandford, R. D. and Znajek, R. L. (1977), Electromagnetic extraction of energy from Kerr black holes, *Monthly Notices of the RAS*, **179**, pp. 433–456.

Cremaschini, C., Kovář, J., Slaný, P., Stuchlík, Z. and Karas, V. (2013), Kinetic Theory of Equilibrium Axisymmetric Collisionless Plasmas in Off-equatorial Tori around Compact Objects, *Astrophysical Journal, Supplement*, **209**, 15, arXiv: 1309.3979.

Crinquand, B., Cerutti, B., Dubus, G., Parfrey, K. and Philippov, A. (2020), Synthetic gamma-ray lightcurves of Kerr black-hole magnetospheric activity from particle-in-cell simulations, *arXiv e-prints*, arXiv:2012.09733, arXiv: 2012.09733.

Dadhich, N., Tursunov, A., Ahmedov, B. and Stuchlík, Z. (2018), The distinguishing signature of magnetic Penrose process, *Monthly Notices of the RAS*, **478**(1), pp. L89–L94, arXiv: 1804.09679.

Gammie, C. F., McKinney, J. C. and Tóth, G. (2003), HARM: A Numerical Scheme for General Relativistic Magnetohydrodynamics, *ApJ*, **589**, pp. 444–457, arXiv: astro-ph/0301509.

Kološ, M., Stuchlík, Z. and Tursunov, A. (2015), Quasi-harmonic oscillatory motion of charged particles around a Schwarzschild black hole immersed in a uniform magnetic field, *Classical and Quantum Gravity*, **32**(16), 165009, arXiv: 1506.06799.

Komissarov, S. S. (2004), Electrodynamics of black hole magnetospheres, *Monthly Notices of the RAS*, **350**(2), pp. 427–448.

Kopáček, O., Karas, V., Kovář, J. and Stuchlík, Z. (2010), Transition from Regular to Chaotic Circulation in Magnetized Coronae near Compact Objects, *ApJ*, **722**(2), pp. 1240–1259, arXiv: 1008.4650.

Kovář, J., Slaný, P., Cremaschini, C., Stuchlík, Z., Karas, V. and Trova, A. (2014), Electrically charged matter in rigid rotation around magnetized black hole, *Phys. Rev. D*, **90**(4), 044029, arXiv: 1409.0418.

Kovář, J., Stuchlík, Z. and Karas, V. (2008), Off-equatorial orbits in strong gravitational fields near compact objects, *Classical and Quantum Gravity*, **25**(9), 095011, arXiv: 0803.3155.

Kovář, J., Kopáček, O., Karas, V. and Stuchlík, Z. (2010), Off-equatorial orbits in strong gravitational fields near compact objects—II: halo motion around magnetic compact stars and magnetized black holes, *Classical and Quantum Gravity*, **27**(13), 135006, arXiv: 1005.3270.

Kovář, J., Slaný, P., Cremaschini, C., Stuchlík, Z., Karas, V. and Trova, A. (2016), Charged perfect fluid tori in strong central gravitational and dipolar magnetic fields, *Physical Review D*, **93**, p. 124055.

Kovář, J., Slaný, P., Stuchlík, Z., Karas, V., Cremaschini, C. and Miller, J. C. (2011), Role of electric charge in shaping equilibrium configurations of fluid tori encircling black holes, *Phys. Rev. D*, **84**(8), 084002, arXiv: 1110.4843.

Kozlowski, M., Jaroszynski, M. and Abramowicz, M. A. (1978), The analytic theory of fluid disks orbiting the Kerr black hole., *A&A*, **63**(1-2), pp. 209–220.

McKinney, J. C. and Narayan, R. (2007a), Disc-jet coupling in black hole accretion systems - I. General relativistic magnetohydrodynamical models, *Monthly Notices of the RAS*, **375**(2), pp. 513–530, arXiv: astro-ph/0607575.

McKinney, J. C. and Narayan, R. (2007b), Disc-jet coupling in black hole accretion systems - II. Force-free electrodynamical models, *Monthly Notices of the RAS*, **375**(2), pp. 531–547, arXiv: astro-ph/0607576.

Nakamura, M., Asada, K., Hada, K., Pu, H.-Y., Noble, S., Tseng, C., Toma, K., Kino, M., Nagai, H., Takahashi, K., Algaba, J.-C., Orienti, M., Akiyama, K., Doi, A., Giovannini, G., Giroletti, M., Honma, M., Koyama, S., Lico, R., Niinuma, K. and Tazaki, F. (2018), Parabolic Jets from the Spinning Black Hole in M87, *ApJ*, **868**(2), 146, arXiv: 1810.09963.

Novikov, I. D. and Thorne, K. S. (1973), Astrophysics of black holes., in C. Dewitt and B. S. Dewitt, editors, *Black Holes (Les Astres Occlus)*, pp. 343–450.

Pánis, R., Kološ, M. and Stuchlík, Z. (2019), Determination of chaotic behaviour in time series generated by charged particle motion around magnetized Schwarzschild black holes, *arXiv e-prints*, arXiv:1905.01186, arXiv: 1905.01186.

Pugliese, D. and Stuchlík, Z. (2015), Ringed accretion disks: Equilibrium configurations, *The Astrophysical Journal Supplement Series*, **221**, p. 25.

Pugliese, D. and Stuchlík, Z. (2016), Ringed accretion disks: Instabilities, *The Astrophysical Journal Supplement Series*, **223**, p. 27.

Pugliese, D. and Stuchlík, Z. (2017), Ringed accretion disks: Evolution of double toroidal configurations, *The Astrophysical Journal Supplement Series*, **229**, p. 40.

Pugliese, D. and Stuchlík, Z. (2018), Relating kerr smbhs in active galactic nuclei to rads configurations, *Classical and Quantum Gravity*, **35**, p. 185008.

Pugliese, D. and Stuchlik, Z. (2019), Multi-accretion events from corotating and counterrotating SMBHs tori, *arXiv e-prints*, arXiv:1910.03925, arXiv: 1910.03925.

Schroven, K., Trova, A., Hackmann, E. and Lämmerzahl, C. (2018), Charged fluid structures around a rotating compact object with a magnetic dipole field, *Phys. Rev. D*, **98**(2), 023017, arXiv: 1804.11286.

Slaný, P., Kovář, J., Stuchlík, Z. and Karas, V. (2013), Charged Tori in Spherical Gravitational and Dipolar Magnetic Fields, *Astrophysical Journal, Supplement*, **205**, 3, arXiv: 1302.2356.

Stuchlík, Z. (2005), Influence of the RELICT Cosmological Constant on Accretion Discs, *Modern Physics Letters A*, **20**, pp. 561–575, arXiv: 0804.2266.

Stuchlík, Z., Blaschke, M., Kovář, J. and Slaný, P. (2022), Charged fluid nonconducting toroidal structures orbiting a schwarzschild black hole immersed in a split-monopole magnetic field, *Phys. Rev. D*, **105**, p. 103012, URL https://link.aps.org/doi/10.1103/PhysRevD.105.103012.

Stuchlík, Z., Kološ, M. and Tursunov, A. (2019), Magnetized black holes: Ionized keplerian disks and acceleration of ultra-high energy particles, in *Recent Progress in Relativistic Astrophysics*, MDPI, URL https://doi.org/10.3390/proceedings2019017013.

Stuchlík, Z. and Kološ, M. (2016), Acceleration of the charged particles due to chaotic scattering in the combined black hole gravitational field and asymptotically uniform magnetic field, *European Physical Journal C*, **76**, 32, arXiv: 1511.02936.

Stuchlík, Z., Kološ, M., Kovář, J., Slaný, P. and Tursunov, A. (2020), Influence of Cosmic Repulsion and Magnetic Fields on Accretion Disks Rotating around Kerr Black Holes, *Universe*, **6**(2), p. 26.

Stuchlík, Z., Kološ, M. and Tursunov, A. A. (2019), Magnetized black holes: Ionized keplerian disks and acceleration of ultra-high energy particles, *Proceedings*, **17**(1), ISSN 2504-3900, URL https://www.mdpi.com/2504-3900/17/1/13.

Stuchlík, Z., Slaný, P. and Hledík, S. (2000), Equilibrium configurations of perfect fluid orbiting Schwarzschild-de Sitter black holes, *A&A*, **363**, pp. 425–439.

Stuchlík, Z., Slaný, P. and Kovář, J. (2009), Pseudo-Newtonian and general relativistic barotropic tori in Schwarzschild-de Sitter spacetimes, *Classical and Quantum Gravity*, **26**(21), 215013, arXiv: 0910.3184.

Tchekhovskoy, A., McKinney, J. C. and Narayan, R. (2008), Simulations of ultrarelativistic magnetodynamic jets from gamma-ray burst engines, *Monthly Notices of the RAS*, **388**(2), pp. 551–572, arXiv: 0803.3807.

Trova, A., Schroven, K., Hackmann, E., Karas, V., Kovář, J. and Slaný, P. (2018), Equilibrium configurations of a charged fluid around a Kerr black hole, *Phys. Rev. D*, **97**(10), 104019, arXiv: 1803.02262.

Tursunov, A., Stuchlík, Z. and Kološ, M. (2016), Circular orbits and related quasi-harmonic oscillatory motion of charged particles around weakly magnetized rotating black holes, *Phys. Rev. D*, **93**(8), 084012, arXiv: 1603.07264.

Wald, R. M. (1974), Black hole in a uniform magnetic field, *Phys. Rev. D*, **10**, pp. 1680–1685.